



Physical Characterization and Electrical Properties of Sol-Gel-Derived Zirconia Films

Hsin-Chiang You,^a Fu-Hsiang Ko,^{b,*} and Tan-Fu Lei^a

^aInstitute of Electronics Engineering, National Chiao Tung University, Taiwan

^bInstitute of Nanotechnology, National Chiao Tung University, Taiwan

We have developed a simple method for the preparation of ZrO₂ ultrathin films; it involves a sequence of ZrCl₄ precursor preparation in an ice bath, sol-gel spin-coating processing, baking, and annealing. The film thickness was controllable and tunable by altering the ZrCl₄/hexanol ratio. High-resolution transmission electron microscopy (TEM) and thermal desorption spectrometry indicated that the fabricated ultrathin film was thermally stable at annealing temperatures as high as 900°C. Diffraction patterns of TEM indicated that the films obtained at various annealing temperatures were amorphous. Electron spectroscopy for chemical analysis (ESCA) demonstrated an increase in the intensity of the signal for the Zr–O bonds upon increasing the annealing temperature, whereas those for the signals of carbon and chlorine decreased. The ESCA and TEM analyses also suggested that the thickness of the silicon dioxide film increased upon increasing the annealing temperature. The electrical properties, such as the breakdown field (12.5 MV/cm) and the gate current density (<10⁻⁷ A/cm²), of the sol-gel-derived ZrO₂ ultrathin films obtained after annealing at 900°C suggested that they were good electrical insulators. These ZrO₂ thin films are expected to behave as capacitors and as coatings for insulating films.

© 2006 The Electrochemical Society. [DOI: 10.1149/1.2186182] All rights reserved.

Manuscript submitted June 14, 2005; revised manuscript received January 26, 2006. Available electronically April 11, 2006.

Silicon technology has formed the basis of microelectronics and electronics systems for more than 30 years. In terms of productivity, the density of devices on a silicon chip has followed Moore's law, doubling about every two or three years since about 1980. Many researchers are interested in scaling down electronics devices so that they may perform at higher speeds and be prepared at lower costs. Conventional SiO₂ gate dielectrics are reaching their physical thickness limit (1.5 nm); they cannot be used as complementary metal-oxide semiconductor devices because of the high direct-tunneling current and poor reliability. For further scaling of devices, it has been proposed that SiO₂ be replaced by high-*k* dielectric constant materials, such as ZrO₂, HfO₂, Ta₂O₅, Al₂O₃, TiO₂, and silicates (ZrSi_xO_y and HfSi_xO_y).¹⁻⁸ In fact, dielectric films having higher permittivity allow the use of thicker films of equivalent electrical thickness as silicon dioxide; this situation reduces the leakage current and improve the reliability of the dielectric films.

The most important properties of high-*k* dielectric materials that are necessary to maintain continuous increases in device performance and density are their low leakage current, low equivalent oxide thickness (EOT), high breakdown strength, high thermal stability, and gate electrode compatibility. The EOT, t_{eq} , of an alternative high-*k* dielectric can be obtained from the simple equation

$$t_{eq} = (K_{ox}/K_{high-k})t_{high-k}$$

where K_{ox} and K_{high-k} are the dielectric constants of silicon oxide and the high-*k* dielectric, respectively, and t_{high-k} is the physical thickness of the high-*k* material. Future downscaling will require high-*k* materials in which EOT values are reduced to nearly 0.7 nm.⁹ We must bear in mind that many of the characteristics of these high-*k* dielectrics—such as their breakdown mechanism and hysteresis phenomena—are quite different from those of conventional silicon dioxide. When the gate dielectric materials experience high temperatures (>800°C), the thermal stability of the high-*k* dielectric on silicon is an important issue that must be addressed for future metal-oxide-semiconductor field effect transistor devices. The most suitable range of dielectric constants is between 20 and 40. If the material has an extremely high *k*-value (>80), it will induce a large fringing effect. For the purposes of achieving a low leakage current, it is desirable to choose a dielectric material that possesses a large bandgap energy and a large band offset with respect to the Si substrate. ZrO₂ has a dielectric constant of 25, a wide bandgap, good

thermal stability, high hardness, a high melting point, chemical hardness, and a high refractive index.

Recently, numerous technologies have been developed for the preparation of various high-*k* films.¹⁰⁻¹³ Atomic layer deposition (ALD), physical vapor deposition (PVD), and chemical vapor deposition (CVD) methods have all been used to prepare insulating films for new technologies. In the ALD process, ZrCl₄ and H₂O are used to prepare the ZrO₂ films. For the PVD process, a zirconium metal target is used for sputtering under ambient oxygen to deposit the ZrO₂ films. In the CVD method, ZrCl₄ is used as a precursor of the deposited ZrO₂ films.

The sol-gel method is an interesting and simple technique for preparing ceramic films.¹⁴⁻¹⁸ This approach can provide colloidal solvents or precursor compounds when metal halides are hydrolyzed under controlled conditions.¹⁸ In the sol-gel process, hydrolysis, condensation, and polymerization steps occur to form metal oxide networks. These reactions play fateful roles in modifying the final material's properties. The most interesting feature of sol-gel processing is its ability to synthesize new types of materials that are known as "inorganic-organic hybrids." Film formation through spin-coating is a simpler method than using ALD, PVD, or CVD because it requires the cheaper precursors and apparatus. In addition, the film can be fabricated in a normal pressure system instead of under high vacuum. Typically, ZrO₂ is an excellent heat-resistant and chemically durable material that is used, for example, as a material for furnaces.¹⁹ Although ZrO₂ generally provides good electrical insulation, no reports exist that describe the electrical insulation properties of sol-gel-derived ZrO₂ ultrathin films.

In this paper, we applied different annealing conditions to sol-gel ZrO₂ ultrathin films on silicon and used various characterization techniques to evaluate the properties and electrical performances of these deposited films.

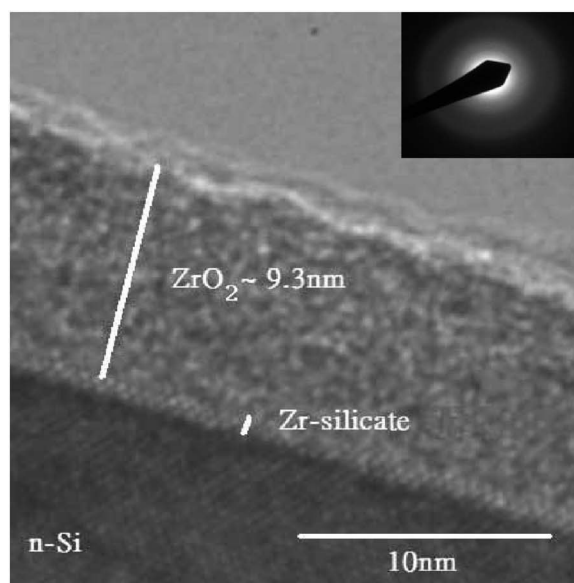
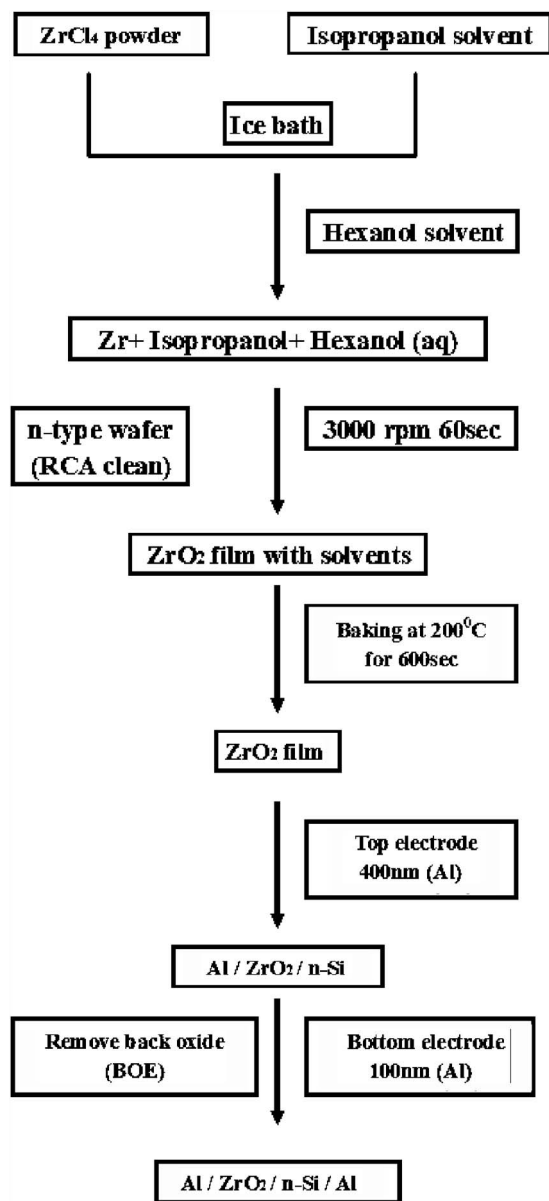
Experimental

The materials were characterized using atomic force microscopy (AFM), electron spectroscopy for chemical analysis (ESCA), X-ray diffractometry (XRD), thermal desorption spectrometry-atmosphere ionization mass spectrometry (TDS-APIMS), and high-resolution transmission electron microscopy (HRTEM). Capacitance–voltage (C–V) and current density–voltage (J–V) analyses were also performed.

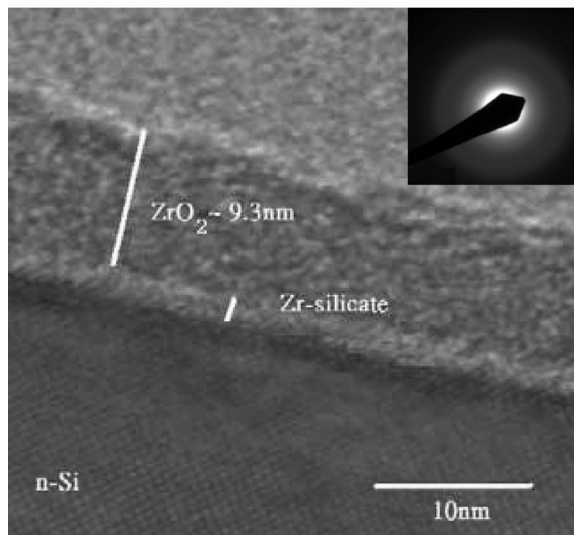
Figure 1 displays the main procedures used for sample preparation. ZrO₂ thin films were prepared using a sol-gel spin-coating method. ZrCl₄ (99.5%, Aldrich, USA) was used as the precursor for the synthesis of zirconia. Prior to film fabrication, the purity of ZrCl₄ was monitored using inductivity coupled plasma optical emis-

* Electrochemical Society Active Member.

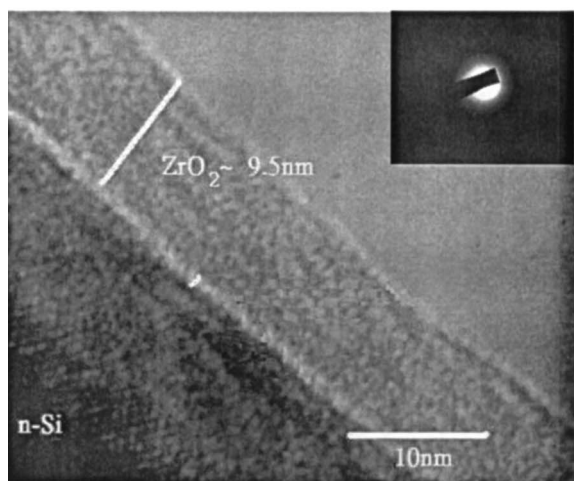
^z E-mail: fhko@mail.nctu.edu.tw



(a)



(b)



(c)

Figure 1. The sol-gel process used for the preparation of ZrO_2 films.

sion spectrometry; apart from the signal for Zr, all other impurities were present at concentrations lower than 1000 ppm. The thin films were prepared through polymerization in an organic solution. A mother sol solution was first prepared by dissolving ZrCl_4 in isopropanol (IPA; Fluka; water content $<0.1\%$) and hexanol (Fluka; water content $<5\%$) under vigorous stirring in an ice bath. The sol solutions were obtained after fully hydrolyzing ZrCl_4 with a stoichiometric quantity of water in IPA and hexanol to yield Zr/IPA/hexanol mixtures with molar ratios of 1:500:1000, 1:500:750, 1:500:500, and 1:500:250. The metal halide solution was then subjected to ultrasonication at 0°C for 20 min to accelerate the gelling rate. The film thickness was determined using the ellipsometer. Film analyses (AFM, ESCA, XRD, TDS-APIMS, TEM, C-V, and J-V) were conducted using the sample having a Zr IPA hexanol molar ratio of 1:500:1000.

The n-type wafers (10–15 Ω cm, made in Japan), which were used as substrates for the metal insulator semiconductor (MIS) structure, were RCA-cleaned to remove the native silicon oxide. ZrO_2 films were deposited by spin-coating at 3000 rpm for 60 s at ambient temperature (25°C) to give a thickness of ca. 9.3 nm on the

Figure 2. Cross-sectional TEM images of sol-gel-derived (Zr + IPA + hexanol) ZrO_2/Si structures annealed under an O_2 atmosphere at (a) 200, (b) 600, and (c) 900°C .

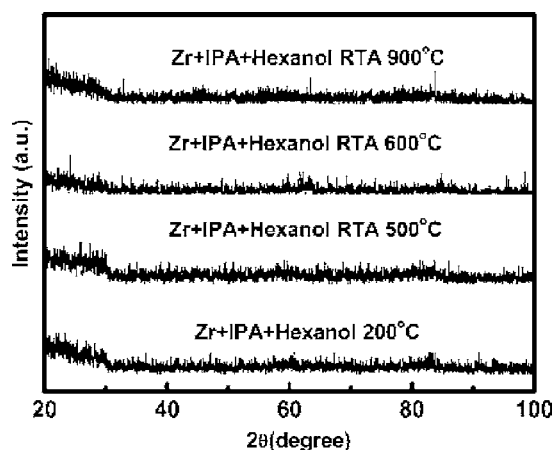


Figure 3. XRD data for ZrO_2 films prepared under different conditions (as-deposited and after annealing at the temperatures indicated).

n-Si(100) substrate. The spin-coater used was a TEL Clean Track model-MK8 (Japan). These films were initially baked at 200°C for 10 min. One of the samples was then maintained at 200°C for 1 min for densification; the others were subjected to rapid thermal annealing (RTA) at different temperatures (500, 600, or 900°C) for 1 min under an oxygen atmosphere. $\text{ZrO}_2/\text{n-Si}$ structures were used in our experiments for the physical characterization of the zirconia.

Next, Al top electrodes having an area of $7.85 \times 10^{-5} \text{ cm}^2$ were deposited onto the top surface of the ZrO_2 by using a shadow mask and vaporizing a pure Al target. The thickness of the top electrode was 400 nm. A buffered oxide etch (BOE) was performed to remove the silicon back oxide and then the sample was thoroughly rinsed with deionized water. Finally, bottom electrodes were attached on the reverse side of the n-Si(100) substrates by vaporizing a pure Al target. The thickness of the bottom electrode was 100 nm. The dielectric properties were then determined for the MIS capacitors having an Al/ $\text{ZrO}_2/\text{n-Si}/\text{Al}$ structure. This deposition technique allows the production of ultrathin gate dielectric films under excellent thickness control.

Results and Discussion

We studied the thicknesses of the smooth ZrO_2 films as a function of the Zr/hexanol ratios. In this sol-gel process, the IPA solvent was more hydrophilic than hexanol. For this reason, we fixed the mole ratio of the IPA solvent with respect to the Zr ions at 1:500 (ZrCl_4/IPA). We varied the hexanol content to provide various film thicknesses. The film thickness increased linearly upon decreasing the Zr/hexanol ratio from 1:1000 to 1:750 to 1:500 to 1:250. We obtained a smooth nanofilm (thickness 9.3 nm) at a Zr/hexanol ratio of 0.001. Prior to annealing, the real thicknesses of the smooth films obtained at Zr/hexanol ratios of 1:750, 1:500, and 1:250 were 10.7, 12.6, and 22.5 nm, respectively. The semi empirical linear fit between the thickness and the Zr/hexanol ratio [thickness $T(\text{nm}) = 4.55 + 4425.90 \times (\text{Zr/hexanol})$ (correlation coefficient: $R^2 = 0.9919$)] suggests that the film thickness is controllable and tunable by altering the Zr/hexanol ratio.

Figure 2a-c displays cross-sectional TEM images of the interfaces of the ZrO_2/Si structures annealed at 200, 600, and 900°C , respectively. The TEM image and its diffraction pattern in Fig. 2a indicate that the sol-gel-deposited film consists of a ca. 0.82-nm interfacial layer and a 9.3-nm-thick bulk ZrO_2 film, and the diffraction pattern suggested that the ZrO_2 exhibited an amorphous structure. Yamaguchi et al.⁹ observed the formation of an interfacial Zr-silicate layer after the pulsed-laser-ablation deposition of ZrO_2 . Wang and co-workers¹¹ also proposed the presence of a Zr-silicate layer after atomic layer chemical vapor deposition of ZrCl_4 . We suggest that the interfacial layer in Fig. 2a may be attributed to such

a Zr-silicate. Very smooth interfaces exist in this sample. When we increased the annealing temperature to 600 and 900°C (Fig. 2b and c), the interfaces were also smooth and the ZrO_2 films remained amorphous in structure, as judged from the diffraction pattern.

We used AFM to evaluate the surface quality of these sol-gel-derived zirconia films. The as-deposited (200°C) sample possessed a whole-area-film root-mean-square (rms) roughness of 0.306 nm. After annealing at 500, 600, and 900°C under ambient oxygen for 1 min, the rms roughnesses were 0.157, 0.165, and 0.189 nm, respectively. The value of the surface roughness of the as-deposited ultrathin film after spin-coating was very low, and these films became even smoother after the annealing treatment. We determined the roughness of each sample at five different regions and found that the annealed samples remained smooth.

Next we investigated the ZrO_2 crystallinity using 1.5° glancing-angle XRD. High- k dielectric crystallinity is a concern because of possible problems arising from leakage paths and dopant/impurity diffusion along grain boundaries, as well as for the control of device uniformity. Figure 3 displays the XRD patterns of the ZrO_2 films. Broad features are present in the XRD pattern of the as-deposited film; they did not change their appearance significantly after annealing at temperatures up to 900°C . These results suggest that the samples have high thermal stability and that RTA treatment at 900°C for 1 min under an oxygen atmosphere does not result in the crystallization of ZrO_2 .

To determine the bulk properties of the deposited films, we used ESCA to examine the nature of the chemical bonding structures of these films. From the Zr 3d spectrum of the RTA samples in Fig. 4a, we observed clearly two typical peaks, Zr $3d_{5/2}$ (183.2 eV) and Zr $3d_{3/2}$ (185.6 eV), of ZrO_2 . RTA annealing under O_2 at 500, 600, and 900°C for 1 min led to remarkable changes in the ESCA spectra (Fig. 4a). The intensities of the signals at 183.2 eV after annealing the as-deposited film at 500, 600, and 900°C were 1.24, 1.32, and 1.48 times higher, respectively, than that after baking at 200°C ; similarly, the peak intensities at 185.6 eV were 1.25, 1.38, and 1.54 times higher, respectively. That is to say, increases in the signals of the Zr–O bonds occur upon increasing the annealing temperature. As-deposited zirconia films exist mainly in the form $\text{ZrO}_{2-\delta}$ ($\delta > 0$). Annealing under ambient oxygen can decrease the value of δ , leading to the formation of ZrO_2 .⁸ The electron binding energy of the C 1s orbital is 284 eV; this value increases to 286.5 eV when Cl is bound to C, as in Fig. 4b.²⁰ The C and Cl atoms both arise from the precursor or the solvents used during the preparation procedure. Annealing at 900°C in the oxygen-rich environment effectively reduces the intensity of the C–Cl signal (cf. Fig. 4b and c). This observation suggests that annealing is beneficial for enhancing the film's quality and improving its electrical properties.

For ESCA analysis, the surfaces of these samples were sputtered away using a 2-kV argon beam (scanning X-ray microprobe, Quantera SXM, ULVAC). Each sample was then eroded ~ 7 nm from the surface. In the spectrum of each RTA sample (Fig. 5), Si 2p peaks appears at 103.3 and 99.3 eV, corresponding to the binding energies of SiO_2 and Si–Si bonds, respectively.⁸ It is obvious that the latter signal represents the silicon substrate. We found that the intensity of the peak representing the Si–O bonds in the annealed thin films increased upon increasing the annealing temperature (Fig. 5). This finding is consistent with our observations above regarding the TEM images (Fig. 2). The color at the interface region (ZrO_2/Si) lightened upon increasing the annealing temperature. This finding suggests that the Zr silicate at the interface led to phase separation at 900°C to form amorphous SiO_2 .⁸

As we mentioned above, C–Cl bonds existed in the ZrO_2 films; annealing at 900°C in the oxygen-rich environment significantly reduced their abundance. To verify this observation, we analyzed these samples through TDS-APIMS measurements. We ramped the desorption temperature of the TDS-APIMS system from room temperature to 800°C at $20^\circ\text{C}/\text{min}$ under a N_2 carrier gas. We analyzed the surface out-gasses at molecular weights of 16, 44, and 82 (Fig.

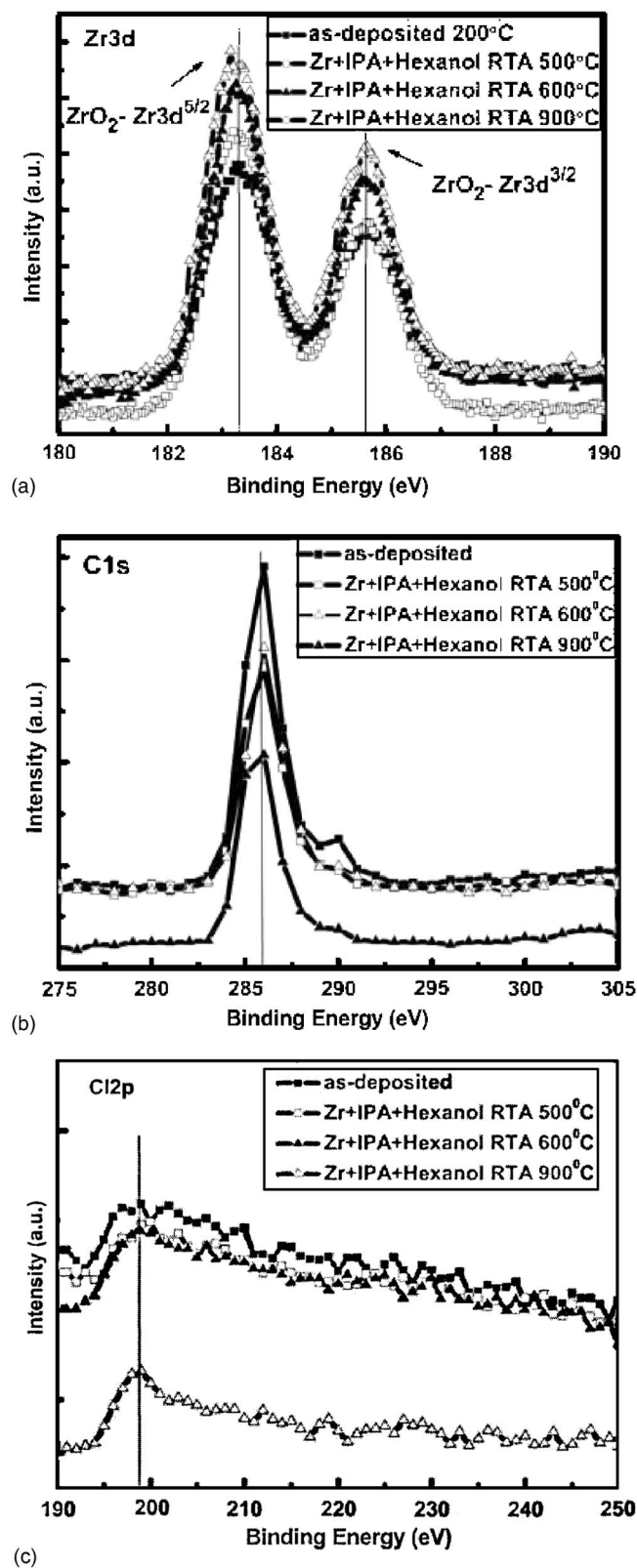


Figure 4. (a) ESCA spectra of as-deposited ZrO_2 films and after RTA annealing at 500, 600, and 900°C in O_2 for 1 min (Zr 3d). ESCA spectra of (b) Cl and (c) C atoms after annealing at different temperatures.

6a-c). The film basically comprises Zr, Cl, C, H, and O elements derived from the preparation solvents and the precursor. The outgassing molecular weights of 16 and 44 possibly represent carbon

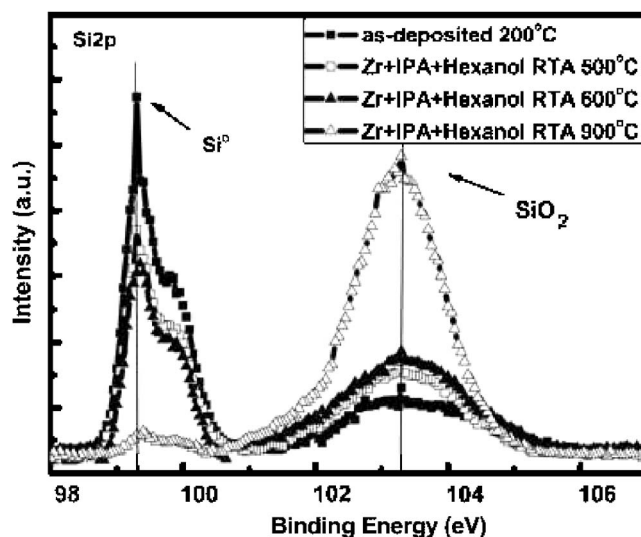


Figure 5. ESCA spectra (Si 2p) of ZrO_2 films eroded by ca. 7 nm using an argon sputter.

elements in the forms CH_4 and CO_2 , respectively. In addition, the chlorine components of the film combined with C atoms to form CCl_2 . We find that the organic elements of all of the samples dissipated violently at temperatures of ca. 400°C. As the annealing temperature increased, the intensity of the TDS-APIMS desorption peak gradually reduced. This result suggests that oxygen treatment at higher temperatures is beneficial for the separation of unstable carbon-containing compounds from the sol-gel-fabricated ultrathin film.

Figure 7 illustrates the high-frequency (1-MHz) capacitance vs gate voltage characteristics ($C-V$ curves) for the MIS capacitors prepared from sol-gel-derived ZrO_2 dielectrics under various annealing conditions. For a high- k dielectric material, high-frequency $C-V$ characteristics are important for calculating the equivalent oxide thickness (EOT). From Fig. 7a, we find that the shape of the $C-V$ curve of the sample annealed at 500°C is poor; several steps exist in the curve, which is not very stable. In other words, the sample annealed at 500°C does not appear to have excellent electrical properties because of the presence of unstable organic compounds remaining in the film. This observation is consistent with our finding in Fig. 4b and 6a. When we raised the annealing temperature, the ZrO_2 films exhibited good electrical properties, i.e., lower current densities and improved capacitance. Figure 7b provides detailed information regarding the sample annealed at 600°C. The value of the capacitance of the RTA 600°C sample was 390 pF; this capacitor appears to be very stable. Table I lists the $C-V$ characteristics of the RTA 600°C sample, which has an EOT value of 3.04 nm and a dielectric constant of 13.9. In addition, Fig. 7b displays hysteresis in the $C-V$ characteristics of the samples in the absence of light. The solid line represents the $C-V$ characteristics after measuring the curve by sweeping the voltage from accumulation to inversion and sweeping back (from +2.0 to -2.0 to +2.0 V); we observe that the shift is only 35 mV. We attribute this small shift to the reduction of unstable carbon-containing compounds after annealing.

The capacitance of the film annealed at 900°C under an O_2 atmosphere was 310 pF (Fig. 7c). Thus, the capacitance of the RTA 900°C sample was lower than that of the RTA 600°C sample. From the ESCA signals of these samples, we find that the intensity of the peak for the Si-O bonds in the annealed thin film increased upon increasing the annealing temperature (see Fig. 5). The interfacial oxide (SiO_2) influences the capacitance and the EOT, which is an undesirable property. Nevertheless, the sol-gel-derived ZrO_2 films annealed at 900°C display (Fig. 8) an improved breakdown field (>12 MV/cm²). Table I lists the $C-V$ characteristics of the sample

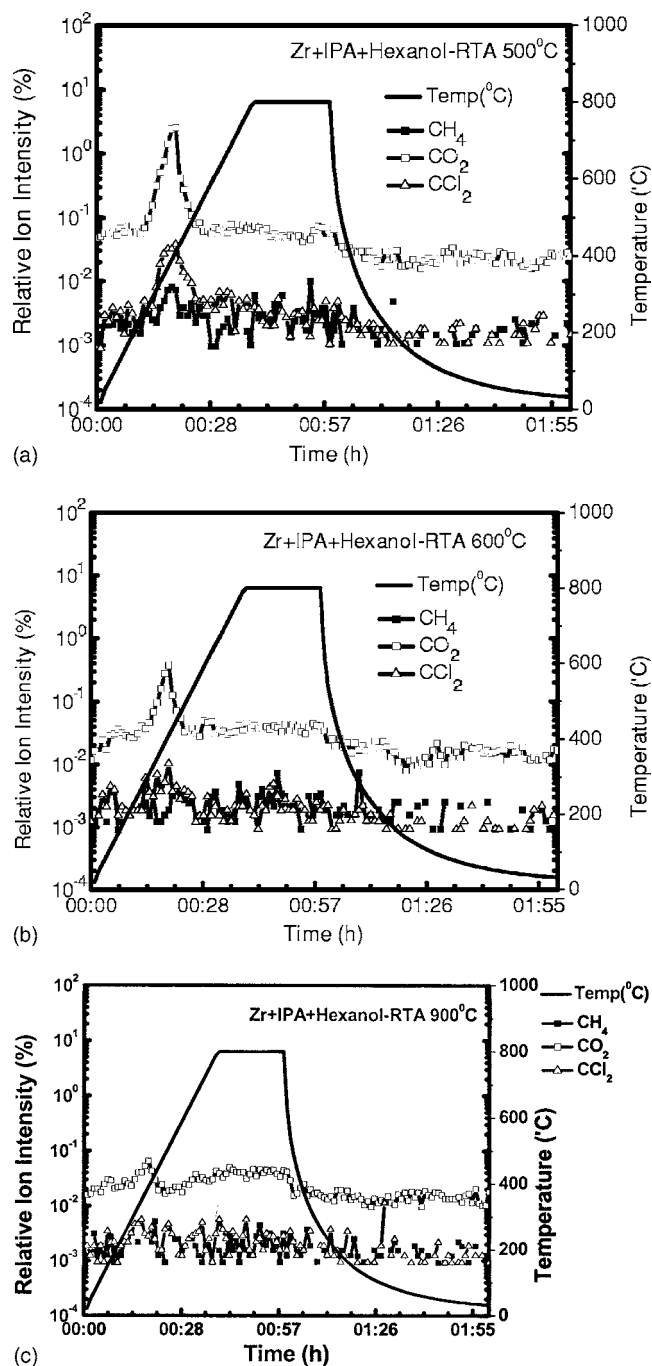


Figure 6. TDS-APIMS analyses of the (a) RTA 500°C, (b) RTA 600°C, and (c) RTA 900°C samples.

annealed at 900°C; the value of EOT was 3.91 nm and the dielectric constant was 12.8. We observe that as the annealing temperature increased, the EOT increased (from 3.07 to 3.91 nm) and the dielectric constant decreased (from 13.9 to 12.8). The solid line in the inset of Fig. 7c represents the C–V characteristics after measuring the curve by sweeping the voltage from accumulation to inversion and sweeping back (from +2.0 to –2.0 to +2.0 V). We observe a shift of 20 mV for the hysteresis phenomenon for the sample annealed at 900°C. Thus, the hysteresis phenomenon is lower than the dielectrics of the sol-gel-derived ZrO₂ film annealed at 600°C.

We obtained the electric field (E) in the J–E curve of Fig. 8 by using the equation $E = V/t_{\text{ox}}$, where V is the applied voltage and t_{ox} is the EOT determined through C–V measurement. The samples

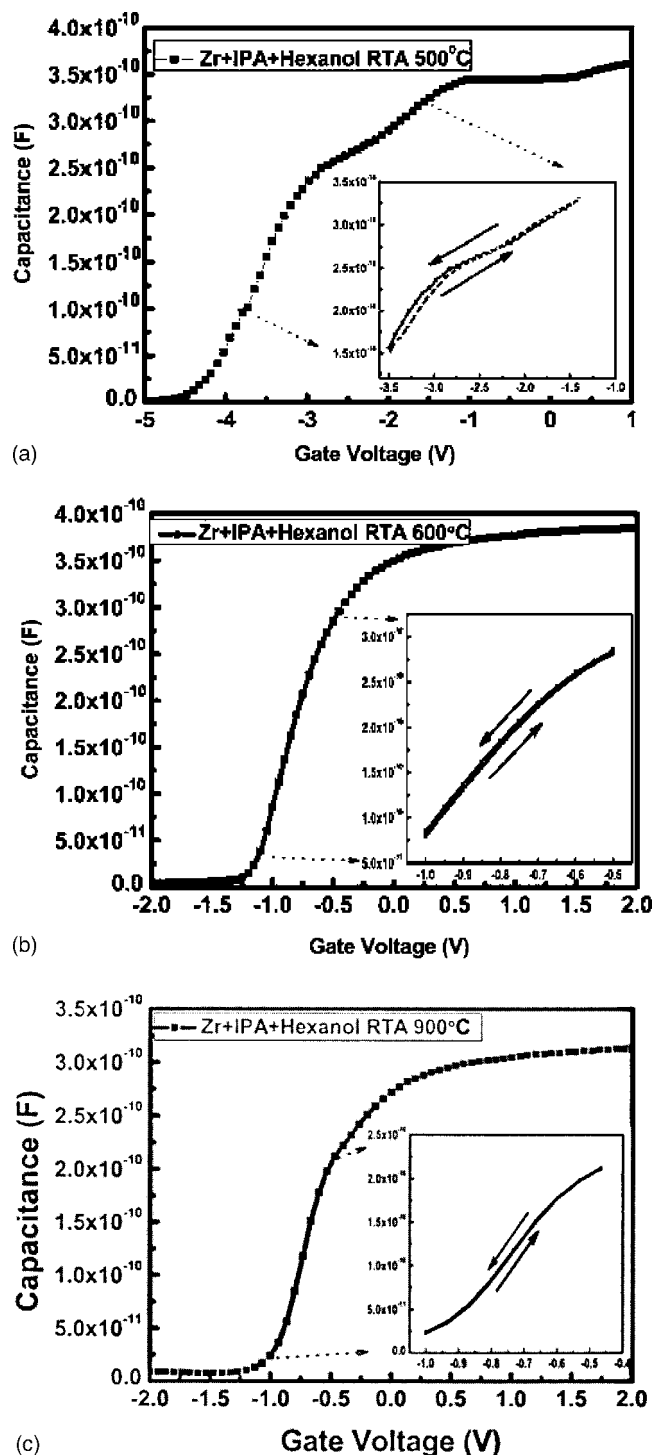


Figure 7. High-frequency (1 MHz) C–V characteristics of the sol-gel-derived ZrO₂ dielectrics after RTA at (a) 500, (b) 600, and (c) 900°C under an O₂ atmosphere.

annealed at 200 and 500°C did not have sufficiently high thermal budgets and thus, their breakdown electric fields were relatively low. The breakdown electric fields increased upon increasing the annealing temperature. A high annealing temperature removed unstable carbon-containing compounds from the ZrO₂ film and stabilized the thin film. The sol-gel-derived ZrO₂ films displayed excellent electrical performances because they did not crystallize during high-temperature RTA, even after annealing at temperatures as high as 900°C. In addition, the samples subjected to RTA treatment at 600

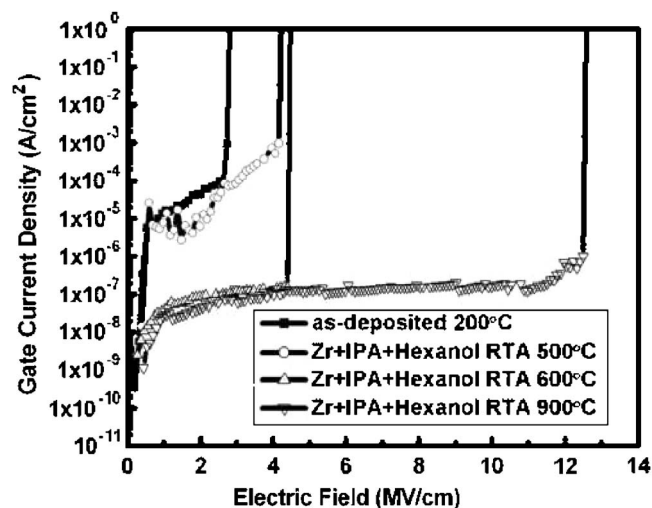


Figure 8. Gate current density vs electric field (J - E) characteristics of the ultrathin film after RTA treatment.

and 900°C displayed leakage current densities ($<10^{-7}$ A/cm²) lower than those reported in the literature for amorphous ZrO₂ films.^{8,11}

Thin layers of zirconium dioxide that are used as dielectrics for capacitors or as gate oxides for MIS devices are subject to a mechanism known as time-dependent dielectric breakdown (TDDB). This mechanism causes the dielectric to break down and electrically short after a certain duration of operation. The expected lifetime of a thin gate oxide under normal operating conditions should be several million years. Figure 9 displays a projected lifetime operation of ca. 1.1 MV/cm for the Zr + IPA + hexanol RTA 500°C sample (five replicate measurements for each point). The projected lifetime operation of the Zr + IPA + hexanol RTA 600°C sample is ca. 2.1 MV/cm, and that of the Zr + IPA + hexanol RTA 900°C sample is ca. 10.4 MV/cm. In this figure, we observe a large increment in the projection voltage for the 10-year lifetime when the Zr + IPA + hexanol sample was annealed at 900°C. This result occurs because the high annealing temperature stabilizes the ZrO₂ film.

Conclusions

In this paper, we propose a sol-gel method for preparing ultrathin films that is attractive because of its low cost and because of the improved thermal and electrical properties of the films. The sol-gel method requires a lower degree of processing and provides highly homogeneous materials; the possibility exists to use annealing processes to stabilize the film. We prepared ZrO₂ ultrathin films of amorphous phase through sol-gel processing using ZrCl₄ as the metal halide. The ZrO₂ thin films not only display good electrical insulation (breakdown fields of up to 12.5 MV/cm) but also improved thermal stability against crystallization (up to 900°C). These

Table I. Properties of films annealed at 600 and 900°C.

Heat-treatment condition	Dielectric constant (k)	EOT (nm)
Zr + IPA + hexanol, RTA 600°C, 1 min	13.9	3.04
Zr + IPA + hexanol, RTA 900°C, 1 min	12.8	3.91

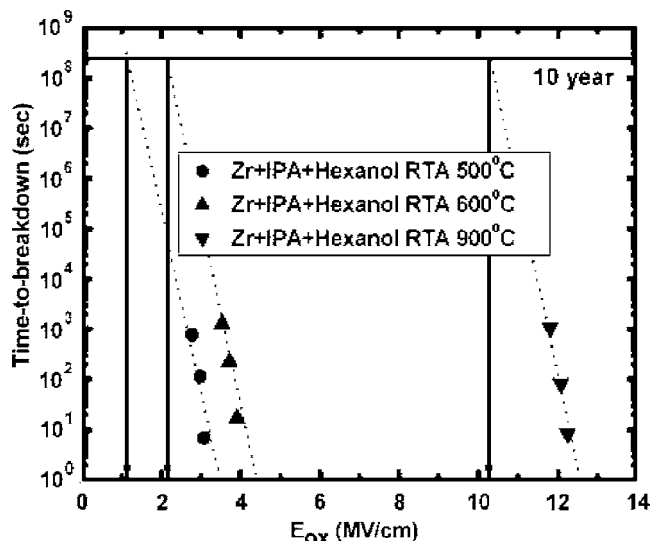


Figure 9. TDDB lifetime projections for the Zr + IPA + hexanol samples after RTA at 500, 600, and 900°C, respectively.

ZrO₂ ultrathin films, which are readily produced, may behave as suitable capacitors and coatings for insulating films.

Acknowledgment

This study was supported financially by the National Science Council, Taiwan, ROC, through contract no. NSC 94-2113-M-009-020.

National Chiaung Tung University assisted in meeting the publication costs of this article.

References

- Y. Ma, Y. Ono, L. Stecker, D. R. Evans, and S. T. Hsu, *Tech. Dig. - Int. Electron Devices Meet.*, **1999**, 149.
- W. J. Qi, R. Nieh, B. H. Lee, L. Kang, Y. Jeon, K. Onishi, T. Ngai, S. Banerjee, and J. C. Lee, *Tech. Dig. - Int. Electron Devices Meet.*, **1999**, 145.
- R. E. Nieh, C. S. Kang, H. J. Cho, K. Onishi, R. Choi, S. Krishnan, J. H. Han, Y. H. Kim, M. S. Akbar, and J. C. Lee, *IEEE Trans. Electron Devices*, **ED-50**, 333 (2003).
- C. H. Lee, H. F. Luan, W. P. Bai, S. J. Lee, T. S. Jeon, Y. Senzaki, D. Roberts, and D. L. Kwong, *Tech. Dig. - Int. Electron Devices Meet.*, **2000**, 27.
- W. J. Qi, R. Nieh, B. H. Lee, K. Onishi, L. Kang, Y. Jeon, J. C. Lee, V. Kaushik, B. Y. Neuyen, L. Prabhu, K. Eisenbeiser, and J. Finder, *VLSI Technical Digest*, p. 40 (2000).
- T. Yamaguchi, H. Satake, and N. Fukushima, *Tech. Dig. - Int. Electron Devices Meet.*, **2001**, 663.
- Z. J. Luo, T. P. Ma, E. Cartier, M. Copel, T. Tamagawa, and B. Halpern, *VLSI Technical Digest*, p. 135 (2001).
- J. Zhu, Z. G. Liu, M. Zhu, G. L. Yuan, and J. M. Liu, *Appl. Phys. A: Mater. Sci. Process.*, **80**, 321 (2005).
- T. Yamaguchi, H. Satake, N. Fukushima, and A. Toriumi, *Tech. Dig. - Int. Electron Devices Meet.*, **2000**, 19.
- Y. Kim, G. Gebara, M. Freiler, J. Barneet, D. Riely, J. Chen, K. Torres, J. Lim, B. Foran, F. Shappur, A. Agarwal, P. Lysaght, G. A. Brown, C. Young, S. Borthakur, H. J. Li, B. Nguyen, P. Zeitzoff, G. Bersuker, D. Derro, R. Bergmann, R. W. Murto, A. Hou, H. R. Huff, E. Shero, C. Pomarede, M. Givens, M. Mazanec, and C. Werkhoven, *Tech. Dig. - Int. Electron Devices Meet.*, **2001**, 455.
- J. C. Wang, S. H. Chiao, C. L. Lee, T. F. Lei, Y. M. Lin, M. F. Wang, S. C. Chen, C. H. Yu, and M. S. Liang, *J. Appl. Phys.*, **92**, 3936 (2002).
- J. P. Chang, Y. S. Lin, and K. Chu, *J. Vac. Sci. Technol. B*, **19**, 1782 (2001).
- J. P. Chang and Y. S. Lin, *J. Appl. Phys.*, **90**, 2964 (2001).
- R. Caruso, A. D. Parralejo, P. Miranda, and F. Guiberteau, *J. Mater. Res.*, **16**, 2391 (2001).
- K. T. Miller and F. F. Lange, *J. Mater. Res.*, **6**, 2387 (1991).
- E. S. González, P. Miranda, A. D. Parralejo, A. Pajares, and F. Guiberteau, *J. Mater. Res.*, **20**, 1544 (2005).
- V. Kiisk, I. Sildos, S. Lange, V. Reedo, T. Tätte, M. Kirm, and J. Aarik, *Appl. Surf. Sci.* **247**, 412 (2005).
- C. J. Brinker and G. W. Scherer, *Sol-Gel Science*, Academic Press, New York (1989).
- A. J. Moulson and J. M. Herbert, *Electroceramics*, Wiley, New York (2003).
- J. C. Vickerman, *Surface Analysis*, Wiley, New York (1997).